Available online at www.sciencedirect.com

ScienceDirect

Catalysis Today 132 (2008) 170–177

CATALYSIS TODAY

www.elsevier.com/locate/cattod

Multi-metal cyanide catalysts for ring-opening polymerization of propylene oxide

Sang Hyun Lee, Seung Hoon Byun, Seung Tae Baek, Hyun Suk Seo,
Dae-Won Park, Chang-Sik Ha, Il Kim *

Division of Chemical Engineering, Pusan National University, Busan 609-735, South Korea

Abstract

Polymerizations of propylene oxide (PO) have been carried out by using a series of multi-metal metal cyanide (MMC) catalysts prepared by reacting $ZnCl_2$ and $K_3[Co(CN)_6]_2$, $K_4Fe(CN)_6$, $K_3Fe(CN)_6$ and/or $K_2Ni(CN)_4$ in the presence of *tert*-butyl alcohol and polytetramethylene ether glycol as complexing agents. The resulting MMC catalysts are characterized by elemental analysis, X-ray photoelectron spectroscopy, infrared spectroscopy and X-ray powder diffraction. The structure of MMC catalysts with broadened X-ray diffraction peaks is different from that of highly crystalline Prussian blue analogues of microporous crystalline materials due to the coordination of complexing agents. The PO polymerization behavior was tunable by changing with various metal cyanide salts after fixing a main catalyst component as $ZnCl_2$. Even if the basic structure of the MMC complexes is different each other, i.e. orthorhombic for $Zn_2[Fe(CN)_6]$ and monoclinic for $Zn_3[Fe(CN)_6]_2$ and $Zn_3[Co(CN)_6]_2$, the chemical formulations become more complicated by forming MMC complexes through cyano bridges and complexing agents' coordination and the structure more distorted from the defined crystal structures. All catalysts prepared by using $K_3[Co(CN)_6]_2$ showed very high activity once they were activated. Simply changing catalyst formulation by choosing different metal cyanide salts, catalytic activity, induction period, polymer molecular weight and its distribution and polymer viscosity could be tuned.

Keywords: Catalysis; Polyol; Propylene oxide; Ring-opening polymerization; Transition metal catalysis

1. Introduction

Multi-metal cyanide (MMC) compounds, the reaction products of a water-soluble metal salt and a water-soluble metal cyanide salt, are well-known catalyst for the polymerization of epoxides and the synthesis of propylene oxide (PO)-based polyether polyols (PPG) which are used in a wide range of polyurethane (PU) applications [1]. The water-soluble metal salt preferably has the general formula MX_2 in which M is selected from the group consisting of Zn^{II}, Fe^{II}, Co^{II} and Ni^{II}. In the formula, X is preferably an anion selected from the group consisting of halide, hydroxide, sulfate, carbonate, cyanide, oxalate, etc. [2–5]. The water-soluble metal cyanide salts used to make the MMC compounds preferably have the general formula $K_aM'(CN)_b$ in which M′ is selected from the group consisting of Co^{II}, Co^{III}, Fe^{II}, Fe^{III}, Cr^{III}, Ir^{III} and Ni^{II}. The water-soluble metal cyanide salt can contain one or more of these metals. Both *a* and *b* are integers greater than or equal to 1 balancing the charge of M. The resulting MMC compounds, Prussian blue analogues, possess structures based upon a simple cubic $M[M'(CN)_6]$ framework, in which octahedral $[M'(CN)_6]^{n-}$ complexes are linked via octahedrally coordinated, nitrogen-bound M^{n+} ions [6,7]. However, these Prussian blue analogues are not active for the polymerization of epoxides. Generally, organic complexing agents such as alcohols are introduced into the catalyst matrix to make them active. The incorporation of the complexing agent makes the catalyst structure and formulation complicated.

Recent improvements have made MMC catalysts much more attractive for commercial manufacture of polyether polyols since they give high-quality PPG products that have low level of unsaturation, narrow molecular weight distribution (MWD) and low viscosity, especially compared to conventional base catalysts [2–3,8–12]. While MMC catalysts offer

---

* Corresponding author. Tel.: +82 51 510 2399; fax: +82 51 512 8563.
E-mail address: ilkim@pusan.ac.kr (I. Kim).

0920-5861/$ – see front matter © 2007 Elsevier B.V. All rights reserved.
doi:10.1016/j.cattod.2007.12.006

attractive advantages over most widely used base catalysts such as KOH and CsOH, they must be activated for a long time before the polymerization starts [3,13–16]. Long induction period, say several hour, increases cycle time and therefore undercuts the economic advantage of faster polymerizations. In addition, heating the catalyst for a prolonged period at high-polymerization temperature above 100 °C can reduce its activity or deactivate it completely [1,9–12].

In order to check the possibility to overcome this shortcoming, the effect of each catalyst component, i.e. M, M′ and complexing agent, on the catalytic behavior for epoxide polymerizations is to be firstly investigated in detail. However, there have been few reports on this topic. Tedious procedures of catalyst preparation together with the inaccessibility of suitable characterization tools of the resulting insoluble catalyst might be the reasons. In a previous report [15] we have shown that the catalytic behavior of the MMC catalysts in PO polymerization prepared by modifying MX_2 to ZnF_2, $ZnCl_2$, $ZnBr_2$ and ZnI_2 changes dramatically. As a continuation of this study, PO polymerizations have been performed with the MMC catalysts prepared by modifying M′ in $K_aM'(CN)_b$ to Co^{III}, Fe^{II}, Fe^{III} and Ni^{II}, fixing MX_2 to $ZnCl_2$ and complexing agents to tertiary butyl alcohol (^{t}BuOH) together with polytetramethylene ether glycol (PTMEG) that is derived from tetrahydrofuran.

2. Experimental

2.1. Material

All materials such as potassium hexacyanocobatate(III) [$K_3Co(CN)_6$], potassium ferrocyanide(II) trihydrate [$K_4Fe(CN)_6{\cdot}3H_2O$], potassium ferricyanide(III) [$K_3Fe(CN)_6$], potassium tetracyanonickelate(II) [$K_2Ni(CN)_4$], zinc chloride ($ZnCl_2$) and ^{t}BuOH were purchased from Aldrich and used without further purification. Polypropylene glycol (molecular weight (MW) = 700; PPG-700) were purchased from Aldrich and used as received. Polymerization grade of propylene oxide (PO) was donated by SKC Company (Korea). Difunctional polypropylene glycol (MW = 700; PPG-700) and PTMEG (MW = 1800) were donated by BASF Korea, Ltd., and used as received after drying (at 110 °C for 6 h under vacuum).

2.2. Preparation of catalysts

A series of MMC catalysts were prepared by using $ZnCl_2$ as a metal salts and $K_3Co(CN)_6$, $K_4Fe(CN)_6{\cdot}3H_2O$, $K_3Fe(CN)_6$ and $K_2Ni(CN)_4$ as metal cyanide salts in the presence of ^{t}BuOH as complexing agent and PTMEG as co-complexing agent. $K_3Co(CN)_6$ (3.32 g, 0.01 mol) was dissolved in distilled water (20 mL) in a beaker (solution 1). $ZnCl_2$ (6.82 g, 0.05 mol) was dissolved in distilled water (50 mL) and ^{t}BuOH (10 mL) in a second beaker (solution 2). A third beaker contained solution 3: a mixture of distilled water (0.5 mL), ^{t}BuOH (10 mL) and PTMEG (2.0 g). Solution 2 was added to solution 1 over 60 min at 50 °C with vigorous mixing using a mechanical stirrer. Solution 3 was then added and the mixture was stirred for 3 min. The mixture was centrifuged. The resulting catalyst (**ZnCo^{III}**) cake was dried at 60 °C under vacuum to a constant weight. The other MMC catalysts using $K_4Fe(CN)_6{\cdot}3H_2O$ (**ZnFe^{II}**), $K_3Fe(CN)_6$ (**ZnFe^{III}**) and $K_2Ni(CN)_4$ (**ZnNi^{II}**) instead of $K_3Co(CN)_6$ were prepared by employing the same procedure keeping the composition of each compound same.

Another series of MMC catalysts were prepared in similar procedures by combining equimolar amounts of $K_3Co(CN)_6$ and $K_4Fe(CN)_6{\cdot}3H_2O$ (**ZnCoFe^{II}**), $K_3Co(CN)_6$ and $K_3Fe(CN)_6$ (**ZnCoFe^{III}**), and $K_3Co(CN)_6$ and $K_2Ni(CN)_4$ (**ZnCoNi^{II}**), keeping the relative compositions of the other compounds and the reaction conditions same.

2.3. Polymerization of propylene oxide

Semi-batch polymerization of PO was carried out by using 1 L autoclave (Parr) at various temperatures. The reactor was charged with 70 g of PPG-700 starter that yields difunctional PPG polyol and the MMC catalyst (0.1 g), and then purged with several time with nitrogen. The mixture was heated to 100 °C and evacuated for over 6 h with vigorous agitation in order to remove traces of water possibly contained in the reaction mixture. Then 15 g of PO monomer was introduced into the reactor at a polymerization temperature (typically 115 °C). Additional monomer was started to add continuously when an accelerated pressure drop, indicating activation of the catalyst, occurred in the reactor. The polymerization was stopped when the total amount of added monomer reached 400 g for a facile agitation. The pressure of the reactor kept constant at 0.7 bar throughout a polymerization run. A clear liquid product was obtained after removal of unreacted monomer under vacuum. The polymerization rate was continuously recorded by measuring the weight of the monomer introduced into the reactor by using personal computer connected with electronic balance through AD converter. To determine reaction rate, a plot of PO consumption (g) versus reaction time (min) was prepared.

2.4. Characterizations

Infrared (IR) spectra were recorded on a Shimadzu IRPrestige-21 spectrophotometer with 32 scans per experiment at a resolution of 1 cm^{-1}. X-ray diffraction (XRD) patterns of the catalysts were obtained with a RINT2000 wide angle goniometer 185 using Cu Kα radiation at 40 kV and 30 mA. Slit sizes were 1° (for the divergence slit), 0.05° (for the monochrometer slit) and 0.15° (for the detector slit). The data were collected from 5° to 70° 2θ with a step size of 0.02° 2θ and a counting time of 3–6 s per step. Elemental analysis was carried out on MMC catalyst. The expected relative error for Zn, Co, Cl, C, H and N is ±3% and oxygen was obtained by subtraction. Elemental analysis of Zn, Co and Cl was obtained by laser ablation inductively coupled plasma mass spectrometry (LA-ICP-MS), on a Agilent 7500 ICP-MS. Elemental analysis for C, H and N was performed by combustion analysis, on a Perkin Elmer CHN Analyzer (Model 2400). For the gas sorption measurements, sample tubes of a known weight were loaded with 200–400 mg of sample and sealed using a transeal.

Samples were degassed at 100 °C for 24 h on a Micromeritics ASAP 2020 analyzer until the outgas rate was no more than 1 mTorr/s. The degassed sample and sample tube were weighed precisely and then transferred back to the analyzer (with the transeal preventing exposure of the sample to air after degassing). The outgas rate was again confirmed to be no more than 1 mTorr/s. Measurements were performed at 77 K in a liquid nitrogen bath.

The total degree of unsaturation of polyols was measured by titration method according to ASTM D2847. Molecular weight (MW) and its distribution (MWD) was measured by gel permeation chromatography (GPC) using a Waters 150 instrument operated at 25 °C, with a set at 10^4, 10^3 and 500 angstroms columns in tetrahydrofuran solvent. Polystyrene standards with low polydispersity were used to generate a calibration curve. The viscosity of polymer was measured at 30 °C. A Brookfield viscometer model DV III (Brookfield Instruments), with a small scale sample adapter and spindle no. 21, was used to measure the viscosity of the polymer samples. The accuracy of viscosity measurement was ±15 cP. A thermostated water bath was used to maintain the temperature of the sample through a water jacket fitted to the small sample adapter. The bath temperature was maintained with an accuracy of ±1 °C. Before performing the experiments, the samples were deaerated. The viscosity measurements were repeated three times each and the averages of the readings were taken for the analysis of the data.

3. Results and discussion

3.1. Catalyst characterization

As one of the oldest known coordination solids, Prussian blue ($Fe_4[Fe(CN)_6]_3 \cdot 14H_2O$) has captivated scientists for nearly three centuries [17,18]. Its synthesis is readily accomplished by the addition of ferric ions to an aqueous solution containing ferrocyanide ions:

$$4[Fe(H_2O)_6]^{3+} + 3[Fe(CN)_6]^{4-} \rightarrow Fe_4[Fe(CN)_6]_3 \cdot 24H_2O \qquad (1)$$

Here, water molecules coordinated to the ferric ions are displaced by nitrogen atoms from the ferrocyanide ions to generate linear Fe^{II}–CN–Fe^{III} bridges and an extended framework based on the face-centered cubic unit cell [19].

When confronted with cyanide as a ligand, a wide selection of metal ions prefer to adopt an octahedral coordination geometry. Consequently, reactions related to reaction (1) above can be used to produce a large family of solids with structures based on the cubic Prussian blue framework [17–19]. As precipitated from aqueous solutions containing no extraneous alkali metal salts, these Prussian blue analogues tend to possess neutral frameworks in which charge balance dictates the number of lattice vacancies. For example, reactions between dications and trianionic hexacyanometalates generate frameworks with a 3:2 stoichiometry and a higher concentration of vacancies than in Prussian blue:

$$3[Zn(H_2O)_6]^{2+} + 2[M'(CN)_6]^{3-} \rightarrow Zn_3[M'(CN)_6]_2 \cdot 18H_2O \qquad (2)$$

In such cases, one-third of all hexacyanometalate units are missing from the unit cell, and again the vacancies are disordered over long range. Reactions of $ZnCl_2$ with $K_3[Co(CN)_6]$ and $K_3[Fe(CN)_6]$ in aqueous solution are expected to give structure of this type [1,13–16]. Thus, the porosity of the metal-cyanide framework in Prussian blue analogues, which directly correlates with the concentration of hexacyanometalate vacancies, is readily manipulated via charge balance. Similarly Reaction between $ZnCl_2$ and $K_4[Fe(CN)_6]$ yields frameworks with a 1:1 stoichiometry:

$$2[Zn(H_2O)_6]^{2+} + [Fe(CN)_6]^{2-} \rightarrow Zn_2[Fe(CN)_6] \cdot 12H_2O \qquad (3)$$

In this case, half of all hexacyanometalate units are missing from the unit cell. In addition the X-ray powder pattern is different from those of other cubic hexacyanides shown above and was indexed assuming an orthorhombic unit cell [20]. The orthorhombic unit cell shows a hexagonal pseudosymmetry. A similar type relation observed for cubic hexacyanide structures which consist of a unit cell in which the equivalent positions are partly occupied by metallic ions, probably holds for orthorhombic $Zn_2[Fe(CN)_6]$ and monoclinic $Zn_3[Fe(CN)_6]_2$ [20].

Reactions between zinc dication and dianionic tetracyanonickelate ($K_2[Ni(CN)_4]$) generate frameworks with a 1:1 stoichiometry as well:

$$[Zn(H_2O)_6]^{2+} + [Ni(CN)_4]^{2-} \rightarrow Zn[Ni(CN)_4] \cdot 6H_2O \qquad (4)$$

The crystal structure of the zinc(II)-nickel(II) complex is different from $Zn_3[M'(CN)_6]_2 \cdot xH_2O$ ($M' = Co$, Fe) and $Zn[Fe(CN)_6] \cdot xH_2O$ in that it consists of a one-dimensional polymeric chain –Zn–NC–Ni$(CN)_2$–CN–Zn– in which the Zn^{II} and Ni^{II} atoms are linked to each other by the cyano groups [21].

All Prussian blue analogue compounds, $Zn_3[Co(CN)_6]_2 \cdot xH_2O$, $Zn_3[Fe(CN)_6]_2 \cdot xH_2O$, $Zn_2[Fe(CN)_6] \cdot xH_2O$ and $Zn[Ni(CN)_4] \cdot xH_2O$, prepared in aqueous solution according to the reported procedures [22–24], were stable and highly crystalline. However, unfortunately, they gave no activity in PO polymerizations. In order to activate them for PO polymerizations, complexation of suitable organic complexing agents other than water molecules is needed. In this study ^{t}BuOH was used as a complexing agent together with PTMEG. It is expected that the incorporation of these complexing agents makes the composition complicated and the stable crystalline structure collapsed. Insoluble nature of the resulting complexes makes the detailed spectroscopic analysis difficult. Table 1 shows results of elemental analysis and approximate empirical formulas for seven catalysts. Since the ligands are consisted of water, ^{t}BuOH and PTMEG, it was impossible to assign relative amounts of each compound based on elemental analysis. For these seven cases, Zn/Co^{II}, Zn/Fe^{III}, Zn/(Co^{III} + Fe^{III}), Zn/Fe^{II}, Zn/(Co^{III} + Fe^{II}), Zn/Ni^{II} and

Table 1
Elemental analysis (wt%) of multi-metal cyanide catalysts prepared by reacting $ZnCl_2$ and $K_3[Co(CN)_6]_2$, $K_4Fe(CN)_6$, $K_3Fe(CN)_6$ and/or $K_2Ni(CN)_4$ in the presence of *tert*-butyl alcohol and polytetramethylene ether glycol as complexing agents

Catalysts	Molar ratio in feed			Element analysis in wt%								
	Co/Fe^{III}	Co/Fe^{II}	Co/Ni^{II}	Zn	Co	Fe	Ni	C	H	O	N	Cl
$Zn_{2.4}Cl_{1.0}[Co(CN)_6]_{1.0}$·ligands[a]												
$ZnCo^{III}$				16.1	6.2			39.4	8.5	16.5	9.0	4.1
$Zn_{2.1}Cl_{0.8}[(0.6Co(CN)_6)\cdot(0.4Fe(CN)_6)]_{1.0}$·ligands												
$ZnCoFe^{III}$	5/5			15.5	3.9	2.6		40.2	10.6	15.6	8.4	3.2
$Zn_{2.7}Cl_{1.3}[Fe(CN)_6]_{1.0}$·ligands												
$ZnFe^{III}$	0/10			16.8		5.3		38.3	8.2	18.3	8.6	4.5
$Zn_{2.1}Cl_{0.9}[(0.5Co(CN)_6)\cdot(0.5Fe(CN)_6)]_{1.0}$·ligands												
$ZnCoFe^{II}$		5/5		16.6	3.7	3.3		37.5	7.1	17.5	10.3	4.0
$Zn_{2.3}Cl_{1.0}[Fe(CN)_6]_{1.0}$·ligands												
$ZnFe^{II}$		0/10		22.1		8.2		34.9	10.6	10.4	8.7	5.1
$Zn_{2.2}Cl_{0.9}[(0.5Co(CN)_6)\cdot(0.5Ni(CN)_4)]_{1.0}$·ligands												
$ZnCoNi^{II}$			5/5	20.8	4.4		4.1	34.0	9.7	14.1	8.2	4.7
$Zn_{2.0}Cl_{0.8}[Ni(CN)_4]_{1.0}$·ligands												
$ZnNi^{II}$			0/10	19.6			8.6	34.8	9.8	14.1	8.8	4.3

[a] Ligands consisting of $x^tBuOH\cdot yH_2O\cdot H\cdot zPTMEG$. Assignment of x, y and z values was impossible due to the complicated composition of the complexes.

$Zn/(Co^{II} + Ni^{II})$ mole fractions range from 2.0 to 2.4. The presence of chlorine atom ranging from 3.2 to 5.1 wt% demonstrates that all catalysts contain appreciable amounts of free $ZnCl_2$.

Fig. 1 shows XRD curves of seven of the catalysts, including $Zn_3[Co(CN)_6]_2\cdot 12H_2O$ prepared in aqueous solution according to the reported procedures [22]. The X-ray powder diffraction pattern [Fig. 1(a)] of the Prussian blue analogue, $Zn_3[Co(CN)_6]_2\cdot 12H_2O$ that is inactive for PO polymerization, was fully consistent with the usual Prussian blue structure type, displaying sharp, intense peaks featuring cubic phase. However, the MMC compounds prepared by using ^{t}BuOH and PTMEG as complexing agents in the presence of excess amount of $ZnCl_2$ showed significantly broadened peaks, suggesting a much smaller crystallite size and/or a lowering of the crystalline order. Comparing **$ZnCo^{III}$** to **$ZnFe^{III}$** catalyst, the latter shows a higher crystallinity. The MMC compounds prepared by reacting excess Zn^{II} with Fe^{II} and Ni^{II} in the presence of organic complexing agents are characterized by more broadened XRD curves, demonstrating the expected structures, orthorhombic $Zn_2[Fe(CN)_6]$ and one-dimensional polymeric $Zn[Ni(CN)_4]$, are much more disordered. The broadened peaks make it difficult to assign cell parameters and thus to characterize the exact structural forms.

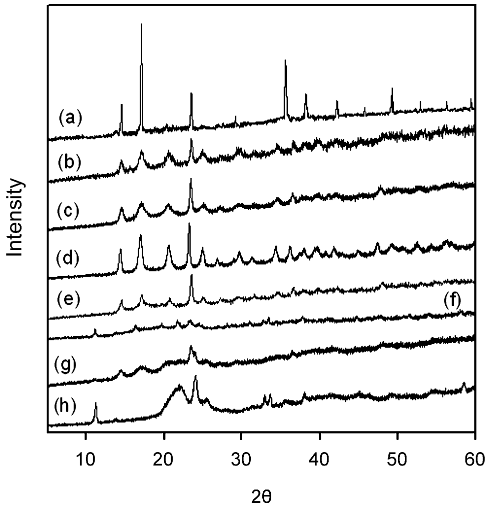

Fig. 1. X-ray powder diffraction patterns of (a) $Zn_3[Co(CN)_6]_2\cdot 12H_2O$ and MMC catalysts bearing *tert*-butyl alcohol and polytetramethylene ether glycol as complexing agents: (b) $ZnCo^{III}$, (c) **$ZnCoFe^{III}$**, (d) **$ZnFe^{III}$**, (e) **$ZnCoFe^{II}$**, (f) **$ZnFe^{II}$**, (g) **$ZnCoNi^{II}$** and (h) **$ZnNi^{II}$** catalysts.

XPS is sensitive to detect the chemical composition of the surface structures so that it is a good tool to characterize insoluble catalysts. Table 2 summarizes the results of XPS analysis of the MMC catalysts together with the starting materials. Relative atomic percentage of each element existed on the surface obtained by the integration of the peaks agrees well with the results of elemental analysis. The binding energy of zinc atom (the 2p3 XPS line at 1023.7 eV) in $ZnCl_2$ shifted to lower values, 1021.3 eV for **$ZnCo^{III}$** and 1017.5 eV for **$ZnFe^{II}$**, respectively. These shifts are related to the formation of zinc cyanocobaltate-based compounds. As the electron withdrawing power of the ligands bound to Zn atom decreases due to the substitution of Cl for CN ligands and at the same time the coordination of complexing agents to coordinatively unsaturated Zn metal centers led to the chemical shift to lower values. It is noted that there exist considerable amounts of free zinc halides (as Cl 2p3) already demonstrated by elemental analysis. The C 1s peak coming from the carbon element was taken as an internal reference and its BE value set at 283.0 eV. Peak assigned to Co 2P3 in $K_3Co(CN)_6$ shifts from 781 eV to slightly lower binding energy by 0.6 eV for **$ZnCo^{III}$** and by 2.6 eV for

Table 2
XPS and IR analyses of multi-metal cyanide catalysts

Compound	XPS analysis results[a]																IR analysis (cm^{-1})		
	Zn 2p3		Co 2p3		Fe 2p3		Ni 2p3		O 1s		N 1s		C 1s		Cl 2p		ν(CN)	ν(MtC)	ν (MtCN)
	B.E (eV)	AT (%)	B.E (eV)	AT (%)	B.E (eV)	AT (%)	B.E (eV)	AT (%)	B.E (eV)	AT (%)	B.E (eV)	AT (%)	B.E (eV)	AT (%)	B.E (eV)	AT (%)			
$ZnCl_2$	1023.7																		
$K_3Co(CN)_6$			781.0														2131	565.1	416.6
$K_3Fe(CN)_6$					709.6												2118	586.4	398.5
$K_4Fe(CN)_6$					707.2												2042	586.4	416.6
$K_2Ni(CN)_4$							853.9										2126		418.6
ZnCo^{III}	1021.3	4.6	780.4	2.2					530.1	18.8	396.7	12.0	283.0	60.1	198.0	2.3	2097	644.2	436.3
ZnCoFe^{III}	1020.2	4.3	779.3	1.2	706.9	0.9			529.7	15.3	395.4	16.7	283.0	60.0	197.2	1.6	2191, 2102	599.9	472.6
ZnFe^{III}	1019.6	5.2			708.2	2.4			530.7	15.8	396.1	13.5	283.0	61.0	196.2	2.1	2096	609.5	474.5
ZnCoFe^{II}	1021.6	4.7	777.8	1.2	706.7	1.1			528.8	20.2	396.3	13.4	283.0	57.4	197.8	2.0	2193, 2101	644.2	472.6
ZnFe^{II}	1017.5	6.3			715.6	3.0			527.2	16.3	396.3	13.9	283.0	57.5	197.6	3.0	2097	624.9	493.8
ZnCoNi^{II}	1021.1	6.5	778.4	1.6			856.5	1.4	529.4	18.0	396.0	12.0	283.0	57.8	196.9	2.7	2193, 2100	644.2	462.9
ZnNi^{II}	1019.7	6.0					855.8	2.6	527.8	17.8	395.8	11.7	283.0	59.5	197.4	2.4	2193	644.2	459.1

[a] Powder pellet in which the calibration was done with the C 1s peak of cyano groups taken at 286.4 eV.

ZnCoNi^{II}. Peak assigned to Fe 2p3 in $K_3Fe(CN)_6$ shifts from 709.6 eV to lower binding energy as well by 1.4 eV for **ZnFe^{III}** by 2.7 eV for **ZnCoFe^{II}**. However, the binding energies of Fe 2p3 in $K_4Fe(CN)_6$ (707.2 eV) and Ni 2p3 in $K_2Ni(CN)_4$ (853.9 eV) shifts to higher ones, 715.6 eV for **ZnFe^{II}** and 855.8 eV for **ZnNi^{II}**, respectively. These red and blue shifts of binding energy indicate a change of microenvironments for the corresponding metal elements.

The formation of cyano bridged complexes can be identified easily since they exhibit sharp ν(CN) at 2200–2000 cm^{-1} (Table 2). The ν(CN) of free CN^- is 2080 cm^{-1} (aqueous solution). Upon coordination to a metal the ν(CN) shifts to higher frequencies. In general the CN^- ion acts as a σ-donor by donating electrons to the metal and also as a π-acceptor by accepting electrons from the metal. σ-Donation tends to raise the ν(CN) band since electrons are removed from the 5σ orbital, which is weakly antibonding, while π-back-bonding tends to decrease the ν(CN) because the electrons enter into the antibonding $2p\pi^*$ orbital. In general, CN^{-1} is a good σ-donor and a poor π-acceptor. Thus the ν(CN) of the complexes are generally higher than the value for free CN^-. The ν(CN) shift of cyano complexes are governed by the electronegativity and the oxidation state of the metal [25]. As summarized in Table 2, the ν(CN) bands in $K_3Co(CN)_6$, $K_3Fe(CN)_6$, $K_4Fe(CN)_6$ and $K_2Ni(CN)_4$ shift to 2131, 2118, 2042 and 2126 cm^{-1}, respectively. Thus the effect of electronegativity is expected in the order $[Co(CN)_6]^{3-} > [Ni(CN)_4]^{2-} > [Fe(CN)_6]^{3-} > [Fe(CN)_6]^{2-}$. Considering the electronegativity of $[Fe(CN)_6]^{2-}$ is smallest, the σ-donation will be the least, and the ν(CN) is expected to be the lowest. Comparing $[Fe(CN)_6]^{3-}$ to $[Fe(CN)_6]^{2-}$, the higher oxidation state, the stronger the σ-bonding, and the higher the ν(CN).

The ν(CN) band shifts further by forming MMC complexes with zinc metal. The ν(CN) bands in **ZnCo^{III}**, **ZnFe^{II}** and **ZnNi^{II}** shift to 2193, 2097, 2193 cm^{-1}, respectively, and that in **ZnFe^{III}** to 2096 cm^{-1}. These shifts of the cyano stretching vibration are another evidence for the formation of new cyano bridges by substituting potassium atoms for zinc atoms. For example, the nickel atom has a square-planar arrangement with four cyanide-carbon atoms where two cyano groups are in terminal position and two further ones in a bridging position. The zinc atom has a distorted octahedral arrangement with two cyano and complexing agents. The cyano ligand acts as N-donor ligand and oxygen atoms in complexing agents are involved in the coordination. Even if the basic structure of the MMC complexes is different from each other, orthorhombic for $Zn_2[Fe(CN)_6]$ and monoclinic for $Zn_3[Fe(CN)_6]_2$ and $Zn_3[Co(CN)_6]_2$, similar complexations are expected to be occurred, so that the chemical formulations become more complicated and the structure more distorted from the defined crystal structures. The MMC complexes, **ZnCoFe^{III}**, **ZnCoFe^{II}** and **ZnCoNi^{II}**, are expected to become even more complicated.

3.2. PO polymerization

In order to investigate the performance of the MMC catalysts for the ring-opening polymerization of PO, semi-batch polymerizations were carried out by using various catalysts at 115 °C. Fig. 2 shows PO consumption versus time curves obtained by **ZnCo^{III}**, **ZnCoFe^{III}**, **ZnFe^{III}**, **ZnCoFe^{II}**, **ZnFe^{II}**, **ZnCoNi^{II}** and **ZnNi^{II}** catalysts. Simple modification of the catalyst formulation by diversifying metal cyanide salts results in great changes in catalytic activity. Comparing the activities obtained by **ZnCo^{III}**, **ZnFe^{III}**, **ZnFe^{II}** and **ZnNi^{II}** catalysts, it can be seen that the efficiency of the metal cyanide salt to form active MMC catalyst decreases $[Co(CN)_6]^{3-} \gg [Fe(CN)_6]^{3-} > [Ni(CN)_4]^{2-} > [Fe(CN)_6]^{2-}$. Table 3 summarizes the polymerization results. The structural electronic changes of the MMC catalysts imposed by different metal cyanide salts of different structure and electronegativity cause such a great change in activity. Taking a look at the curves obtained by **ZnCoFe^{III}**, **ZnCoFe^{II}** and **ZnCoNi^{II}** catalysts prepared by mixed metal cyanide salts, all catalysts give very high activities even if **ZnCoFe^{III}** catalyst shows somewhat declined activity at the later part of polymerization. It is interesting to note **ZnCoFe^{II}** catalyst shows much higher activity than **ZnFe^{II}** catalyst.

Taking a look at the polymerization rate profiles carefully, it can be seen that it needs a long-induction period before polymerization starts. The induction period decreases in the order of **ZnCo^{III}** (93 min) > **ZnCoNi^{II}** (68 min) > **ZnCoFe^{II}** (39 min) > **ZnFe^{III}** (34 min) > **ZnNi^{II}** (12 min) > **ZnCoFe^{III}** (10 min) > **ZnFe^{II}** (9 min). Evidently the prolonged induction period is not attractive as an effective catalyst, since the long-induction period undercuts the economic advantage of the MMC-catalyzed polymerizations. Considering both activity and induction period, it can be seen that the utilization of mixed metal cyanide salts are one of the ways to tune the polymerization behavior the MMC catalysts.

The production of the polyols with ultra low unsaturation contents is one of the crucial benefits of MMC catalysts over conventional base catalyst. It is well known that base catalyzes not only the addition of PO to the growing polymer chain, but also a side reaction in which propylene oxide isomerizes to allyl alcohol [15,16]. Allyl alcohol acts as a monofunctional starter resulting in the production of the propoxylated allyl alcohol, often referred to as monol. The monols are also generated by other types of side reactions [15,16]. The similar side reactions are possible in MMC catalysts especially at high temperatures. In addition high temperature is not favorable to get high-MW polyols. In this sense PO polymerizations were performed at different temperatures (40–130 °C) by using **ZnCo^{III}** and **ZnCoFe^{III}** catalysts and the results are summarized in Table 3. The **ZnCo^{III}** catalyst shows no or negligible activity at $T < 75$ °C. The polymerizations above 120 °C by the same catalyst show considerable decline of activities at the later part of polymerization, most likely due to initial heating of the catalyst for a prolonged period at high temperature for activation. The mixed cyanide **ZnCoFe^{III}** catalyst shows high activities over a broader range of temperature (40–130 °C). It can be an another merit of **ZnCoFe^{III}** catalyst over **ZnCo^{III}** catalyst.

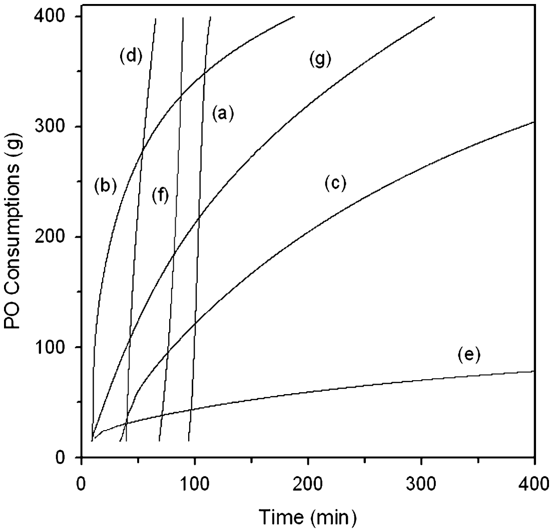

Fig. 2. Polymerization rate curves obtained by using multi-metal catalysts: (a) ZnCo^{III}, (b) **ZnCoFe^{III}**, (c) **ZnFe^{III}**, (d) **ZnCoFe^{II}**, (e) **ZnFe^{II}**, (f) **ZnCoNi^{II}** and (g) **ZnNi^{II}** catalysts. Polymerization conditions: temperature = 115 °C, PPG starter = 70 g and catalyst = 0.1 g.

3.3. Characterization of polymers

Table 3 summarizes characterization results of polymers obtained by various MMC catalysts. As already mentioned, the level of unsaturation contained in polymer is the one of the most important features characterizing MMC catalysts differentiating from conventional base catalysts. Typically KOH catalyzed polyols are characterized by high level of unsaturation (0.03–0.10 meq/g), so that they have limited applications as high performance polyurethane products [1]. As shown in Table 3, the unsaturation value of polyol produced by MMC catalysts bearing $[Co(CN)_6]^{3-}$ as a cyanide salt is much lower than that of polyols produced by base catalysts. The level of unsaturation of all polymers produced by $[Co(CN)_6]^{3-}$ bearing MMC catalysts, **ZnCo^{III}**, **ZnCoFe^{III}**, **ZnCoFe^{II}** and **ZnCoNi^{II}** catalysts is lower than 0.0126 meq/g. Especially the polymer produced at 75 °C by **ZnCo^{III}** catalyst is characterized by extremely low-unsaturation level, 0.0029 meq/g. Comparing polymerization results obtained by **ZnCo^{III}** and **ZnCoFe^{III}** catalysts at different polymerization temperatures, the level of unsaturation increases as the temperature increases, demonstrating side reactions yielding allyl alcohol are activated at high temperatures. It is interesting to note that the choice of metal cyanide salts is a crucial factor to get polymers with low unsaturation level. Simple substitution of metal cyanide salt, $[Co(CN)_6]^{3-}$ for $[Fe(CN)_6]^{3-}$, $[Ni(CN)_4]^{2-}$ or $[Fe(CN)_6]^{2-}$ makes the resulting catalyst yield polymers with relatively high-unsaturation level as well as low the catalytic activity. The level of unsaturation of polymers obtained at 115 °C by **ZnCo^{III}**, **ZnFe^{III}**, **ZnNi^{II}** and **ZnFe^{II}** catalysts is 0.005, 0.0203, 0.017 and 0.0211 meq/g, respectively. It means that **ZnFe^{III}**, **ZnNi^{II}** and **ZnFe^{II}** catalysts lose their own merit as MMC catalysts over conventional base catalysts. From above results it may be said that the use of $[Co(CN)_6]^{3-}$ as a metal cyanide salt is necessary not only to achieve high activity but also to produce polymers with low-unsaturation level.

Table 3
Results of propylene oxide polymerizations by various multi-metal cyanide catalysts

Catalyst	Polymerization temperature (°C)	$R_{\mathrm{p,\ avg}}$ [a]	Induction period (min)	Unsaturation (meq/g)	Viscosity[b] (cP)	M_n [c] (g/mol)	MWD[c]
ZnCo$^{\mathrm{II}}$	115	2667	93	0.0050	1,790	3290	1.31
	95	3870	108	0.0050	1,260	3600	1.07
	75	1800	129	0.0029	975	3070	1.14
ZnCoFe$^{\mathrm{III}}$	130	300	5	0.0116	1,675	5220	1.60
	115	837	10	0.0097	2,850	5220	1.63
	95	7632	11	0.0085	9,250	5520	2.69
	75	4092	13	0.0071	120,000	7080	5.53
	60	3210	16	0.0052	910,000	6240	7.16
	50	732	45	0.0048	540,000	4800	4.19
	40	675	57	0.0036	298,000	4060	4.21
ZnFe$^{\mathrm{III}}$	115	195	34	0.0203	95,000	3360	5.69
ZnCoFe$^{\mathrm{II}}$	115	3291	39	0.0089	1,150	3720	1.07
ZnFe$^{\mathrm{II}}$	115	98	9	0.0182	12,000	3890	3.48
ZnCoNi$^{\mathrm{II}}$	115	2610	68	0.0126	1,550	3790	1.06
ZnNi$^{\mathrm{II}}$	115	729	12	0.0170	124,000	3360	1.14

[a] Average rate of polymerization in g-PPO/g-catalyst h.

[b] Measured by Brookfield DV-II + Programmable Viscometer at 25 °C.

[c] Measured by GPC (polystyrene).

The choice of metal cyanide salt influences the polymer MW and especially MWD. The MW of polymers obtained at 115 °C by **ZnCo$^{\mathrm{III}}$**, **ZnFe$^{\mathrm{III}}$**, **ZnNi$^{\mathrm{II}}$** and **ZnFe$^{\mathrm{II}}$** catalysts is in a similar level between 3290 and 3890 g/mol; however, their MWD values change considerably between 1.14 for **ZnNi$^{\mathrm{II}}$** and 5.69 for **ZnFe$^{\mathrm{II}}$** catalyst. Polymers obtained at 115 °C by all catalysts using mixed metal cyanide show narrow MWD less than 1.63. Polymerization results obtained by **ZnCoFe$^{\mathrm{III}}$** at various temperatures show that MW and MWD values are considerably dependent on the polymerization temperature.

The viscosity of polymer is also an important property during handling and reacting with isocyanate compounds. The lower viscosity should be more favorable for handling and reacting. It is expected that the viscosity is dependent on many parameters such as MW, MWD and unsaturation level of polymer (Table 3). It is quite surprising that the viscosity changes by almost 1000 folds from 975 to 910,000 cP. In fact the polymer obtained by **ZnCoFe$^{\mathrm{III}}$** catalyst at 50 °C looks like a gel, while the polymer obtained by **ZnCo$^{\mathrm{II}}$** catalyst at 75 °C is a clear viscous liquid. It is hard to conclude the effect of individual parameter on viscosity, the MWD values of polymer influence polymer viscosity most deeply.

4. Conclusions

A series of multi-metal catalysts; Zn$^{\mathrm{II}}$–Co$^{\mathrm{III}}$, Zn$^{\mathrm{II}}$–Fe$^{\mathrm{III}}$, Zn$^{\mathrm{II}}$–Fe$^{\mathrm{II}}$, Zn$^{\mathrm{II}}$–Ni$^{\mathrm{II}}$, Zn$^{\mathrm{II}}$–Co$^{\mathrm{III}}$–Fe$^{\mathrm{III}}$, Zn$^{\mathrm{II}}$–Co$^{\mathrm{III}}$–Fe$^{\mathrm{II}}$, Zn$^{\mathrm{II}}$–Co$^{\mathrm{III}}$–Ni$^{\mathrm{II}}$, prepared by reacting $ZnCl_2$ with various metal cyanide compounds such as $K_3[Co(CN)_6]_2$, $K_4Fe(CN)_6$, $K_3Fe(CN)_6$ and $K_2Ni(CN)_4$ in the presence of *tert*-butyl alcohol and polytetramethylene ether glycol as complexing agents were used for ring-opening polymerizations of propylene oxide. Highly crystalline MMC complexes with no organic complexing agents showed no activity. The formation of catalyst formulation was confirmed by elemental analysis. XRD analysis of the MMC catalysts showed that the coordination of organic complexing agents makes the MMC catalysts have a much smaller crystallite size and/or lower the crystalline order. The formation of catalyst formulation through cyano bridges between Zn and other metals was also confirmed by XPS and IR analyses.

Simple modification of the catalyst formulation by diversifying metal cyanide salts resulted in great changes in catalytic activity. Comparing the activities obtained by **ZnCo$^{\mathrm{III}}$**, **ZnFe$^{\mathrm{III}}$**, **ZnFe$^{\mathrm{II}}$** and **ZnNi$^{\mathrm{II}}$** catalysts, the efficiency of the metal cyanide salt decreased $[Co(CN)_6]^{3-} \gg [Fe(CN)_6]^{3-} > [Ni(CN)_4]^{2-} > [Fe(CN)_6]^{2-}$. The induction period could be tuned by a suitable selection of metal cyanide salts, so that the induction period decreased from 93 min for **ZnCo$^{\mathrm{III}}$** catalyst to 39 min for **ZnCoFe$^{\mathrm{II}}$** without sacrificing activity. The polymer produced at 75 °C by **ZnCo$^{\mathrm{III}}$** catalyst showed by extremely low-unsaturation level, 0.0029 meq/g. In general, the use of $[Co(CN)_6]^{3-}$ as a metal cyanide salt was required to produce polymers with low-unsaturation level and low viscosity.

Acknowledgements

This work was supported by the Basic Research Program (KOSEF), the Brain Korea 21 Project, the Center for Ultra Microchemical Process System (ERC), the National Core Research Center Program from MOST and KOSEF (R15-2006-022-01001-0) and the NRL Program.

References

[1] I. Kim, J.-T. Ahn, C.S. Ha, C.S. Yang, I. Park, Polymer 44 (2003) 3417.

[2] B. Le-Khac, W. Wei, US Patent 6,696,383 (2004).

[3] I. Kim, S. Lee, WO 2004045764 (2004).

[4] E. Bothers, M. Triller, B. Bechtloff, R. Ruppel, WO 2006037541 (2006).

[5] H. Sakurai, S. Ikai, Y. Toyota, H. Fukuda, C. Suzuki, US Patent 7,169,956 (2007).

[6] H.J. Buser, D. Schwarzenbach, W. Petter, A. Ludi, Inorg. Chem. 16 (1977) 2704.

[7] F. Herren, P. Fischer, A. Ludi, W. Haelg, Inorg. Chem. 19 (1980) 956.

[8] H.R. Hinney, D.S. Wardius, US 5,158,922 (1992).
[9] B. Le-Khac, EP 654302 (1995).
[10] B. Le-Khac, US 5,482,908 (1996).
[11] B. Le-Khac, US 5,693,584 (1997).
[12] B. Le-Khac, US 5,714,428 (1998).
[13] I. Kim, J.-T. Ahn, C.-S. Ha, C.-S. Yang, I. Park, Polymer 44 (2003) 3417.
[14] I. Kim, J.-T. Ahn, S.-H. Lee, C.-S. Ha, D.-W. Park, Catal. Today 93-95 (2004) 511.
[15] I. Kim, S.H. Byun, J. Polym. Sci., Part A: Polym. Chem. 43 (2005) 4393.
[16] I. Kim, M.J. Yi, K.J. Lee, D.-W. Park, B.U. Kim, C.-S. Ha, Catal. Today 111 (2006) 292.
[17] A. Ludi, H.U. Güdel, Struct. Bond. 14 (1973) 1.
[18] K.R. Dunbar, R.A. Heintz, Prog. Inorg. Chem. 45 (1997) 283.
[19] H.J. Buser, A. Ludi, W. Petter, D. Schwarzenbach, J. Chem. Soc., Chem. Commun. (1972) 1299.
[20] C. Loos-Neskovic, M. Fedoroff, E. Garnier, Talanta 36 (1989) 749.
[21] G.J. Kubas, L.H. Jones, Inorg. Chem. 13 (1974) 2816.
[22] S.K. Steven, R.L. Jeffrey, J. Am. Chem. Soc. 127 (2005) 6506.
[23] E. Garnier, P. Gravereau, A. Hardy, Acta Cryst. B38 (1982) 1401.
[24] O.V. Mikhailov, T.B. Tatarintseva, N.I. Naumkina, V.A. Kolgina, Russian J. Coord. Chem. 29 (2003) 630.
[25] M.F.A. El-Sayed, R.K. Sheline, J. Inorg. Nucl. Chem. 6 (1958) 187.